

Generation and propagation of partially coherent vortex beams

Shengwei Cui (崔省伟), Ziyang Chen (陈子阳), and Jixiong Pu (蒲继雄)*

College of Information Science and Engineering, Huaqiao University, Xiamen 361021, China

*Corresponding author: bug.swei@163.com

Received August 29, 2013; accepted October 14, 2013; posted online March 25, 2014

Partially coherent vortex beams are generated by the illumination of high-power red-color light-emitting diodes. We investigate the influence of correlation property of partially coherent vortex beams on intensity distribution. The correlation property of partially coherent vortex beams are modulated by adjusting the propagation distance of the incident light. Effects of the topological charge and propagation distance of vortex beams on the intensity are also studied. Experiment results are consistent with theoretical simulations.

OCIS codes: 030.1640, 050.4865, 260.3160, 110.4980.

doi: 10.3788/COL201412.S10301.

Light beams that carry orbital angular momentum (OAM) are called vortex beams. The beams comprise l helical phase fronts, described by a phase term $\exp(il\theta)$; meanwhile, every photon of the light beams carries an OAM of $l\hbar$. Therefore, vortex beams are widely used in information coding, space optical communication and optical tweezers and spanners, etc.^[1-9]. In recent years, partially coherent beams have been studied by researchers because they are influenced by turbulent atmosphere to a lesser extent^[10,11]. Swartzlander, Gbur and Lu have already studied many properties of partially coherent vortex beams^[12-21]. However, most of them are restricted to theoretical research, and the vortex beams are generated by laser beams. In this paper, we focus on the experimental study of partially coherent vortex beams generated by a red-color single-lamp light-emitting diodes (LEDs).

As an important light source in modern optics, LED lamps have following advantages: high efficiency to convert electrical energy into light, high levels of brightness and intensity, high reliability, and long source life. Therefore, LEDs are extensively used in many fields, such as optical fiber communication, lighting, LED display^[17-19]. Compared with lasers, LEDs have low coherent degree and wide spectrum. In this study, red LED light source is introduced to generate partially coherent vortex beams. Influences of coherent length, topological charge and propagation distance of partially coherent vortex beams on the intensity distribution are investigated in detail.

In this paper, we used a high-power red-color single-lamp LED (Cree Company) as light source. Figure 1 shows spectral characters of the LED. The solid line in Fig. 1 represents the experimental result of the spectrum, which shows Gaussian shape with the center wavelength (λ_0) of approximately 625 nm and FWHM (w_λ) of approximately 25 nm. Therefore, we simulated the spectrum by a Gaussian function, which can be expressed as

$$S(\lambda) = \exp\left[\frac{-(\lambda - \lambda_0)^2}{(w_\lambda)^2}\right], \quad (1)$$

where, λ_0 is the center of the Gaussian spectrum. The dashed line in Fig. 1 represents the theoretical simulation of the spectrum according to Eq. (1). As it is observed from Fig. 1, the theoretical simulation is consistent with the experimental observation, which confirms that the spectrum of the LED is a Gaussian line.

Figure 2 shows a schematic representation of the experimental setup. The incident light beam size is

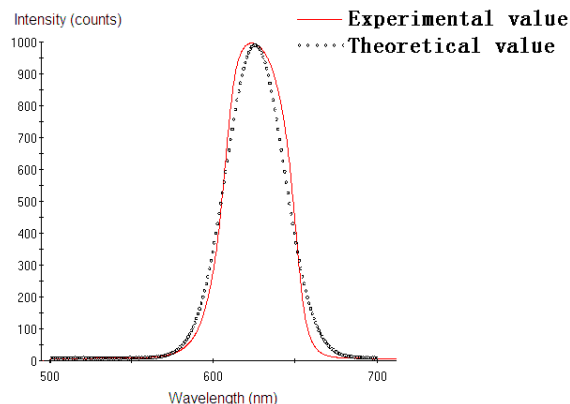


Fig. 1. Experimental and simulated spectra of the red LED. Solid line represents experimental value; whereas dashed line represents theoretical value.

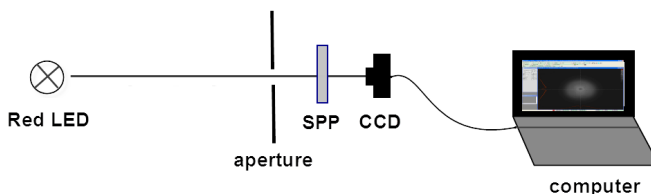


Fig. 2. Experimental setup of generating partial coherence vortex beams using LED.

determined by the aperture. Then, the incident light beams convert to partially coherent vortex beams by passing through a spiral-phase plate (SPP). Charge-coupled device (CCD) is introduced to record the beam patterns. The correlation property of the partially coherent vortex beams can be modulated by adjusting the position of the aperture.

We measured coherent properties by using conventional double-slit interference. Figure 3 depicts the coherent degree of the LED light in Gaussian distribution. Blank dots represent experimental observation, whereas the solid line represents the numerical simulation. The equation can be expressed as

$$\mu(\rho_1, \rho_2, z = 0) = \exp\left\{\frac{-[\rho_1^2 + \rho_2^2 - 2\rho_1\rho_2 \cos(\theta_1 - \theta_2)]}{\delta^2}\right\}, \quad (2)$$

where, δ is coherent length (waist width of Gaussian distribution). The numerical simulation coincides with the experimental observation.

The cross-spectral density of partially coherent vortex beams can be written as

$$W(\rho_1, \rho_2, \theta_1, \theta_2, z = 0) = S(\lambda) \left(\frac{\rho_1}{w}\right)^l \left(\frac{\rho_2}{w}\right)^l \exp\left(-\frac{\rho_1^2 + \rho_2^2}{w^2}\right) \times \exp\left\{\frac{-[\rho_1^2 + \rho_2^2 - 2\rho_1\rho_2 \cos(\theta_1 - \theta_2)]}{\delta^2}\right\} \exp[-il(\theta_1 - \theta_2)], \quad (3)$$

where, w and l are the spot size and topological charge, respectively. Based on the propagation law of cross-spectral density, after a propagation distance of z in free space, the cross-spectral density function of partial coherent vortex beams from LED is given as^[16]

$$W(r_1, r_2, \theta_1, \theta_2, z) = \int \left(\frac{1}{\lambda z}\right)^2 \iiint \iiint W(\rho_1, \rho_2, \theta_1, \theta_2, z = 0) \times \exp\left\{-\frac{i\pi}{\lambda z}[(\rho_1^2 + r_1^2 - 2\rho_1 r_1 \cos(\theta_1 - \varphi_1)) - (\rho_2^2 + r_2^2 - 2\rho_2 r_2 \cos(\theta_2 - \varphi_2))]\right\} \rho_1 \rho_2 d\rho_1 d\rho_2 d\theta_1 d\theta_2 d\lambda. \quad (4)$$

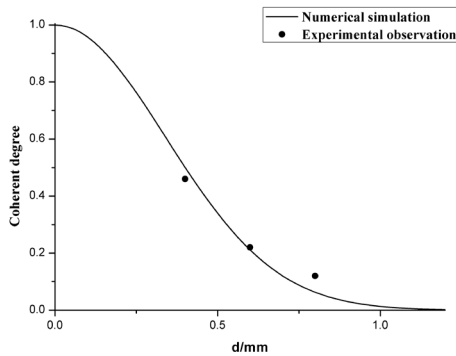


Fig. 3. Correlation property of the red LED. The solid line represents numerical simulation, whereas blank dots represent experimental observation.

Equation (4) can be further simplified as

$$W(r_1, r_2, \varphi_1, \varphi_2, z) = \int \left(\frac{2\pi}{\lambda z}\right)^2 \exp\left[-\frac{i\pi}{\lambda z}(r_1^2 - r_2^2) - \frac{(\lambda - \lambda_0)^2}{(w_\lambda)^2}\right] \sum_{m=-\infty}^{\infty} \iint \left(\frac{\rho_1}{w}\right)^l \left(\frac{\rho_2}{w}\right)^l \exp\left[-\left(\frac{1}{w^2} + \frac{1}{\delta^2}\right)(\rho_1^2 + \rho_2^2)\right] \times \exp\left[-\frac{i\pi}{\lambda z}(\rho_1^2 - \rho_2^2)\right] J_m\left(\frac{2\pi\rho_1 r_1}{\lambda z}\right) J_m\left(\frac{2\pi\rho_2 r_2}{\lambda z}\right) I_{l+m}\left(\frac{2\rho_1\rho_2}{\delta^2}\right) \times \exp[-im(\varphi_1 - \varphi_2)] \rho_1 \rho_2 d\rho_1 d\rho_2 d\lambda. \quad (5)$$

Considering $r_1 = r_2 = r$, $\varphi_1 = \varphi_2 = \varphi$, the intensity distribution of partially coherent vortex beams generated by the LED is expressed as

$$I(r, \varphi, z) = W(r, r, \varphi, \varphi, z). \quad (6)$$

Table 1. The relationship between coherent lengths and propagation distance

Distance (m)	1.5	2.0	2.5	3.0	3.5
Coherent length (mm)	0.4292	0.4811	0.5244	0.7068	0.7808

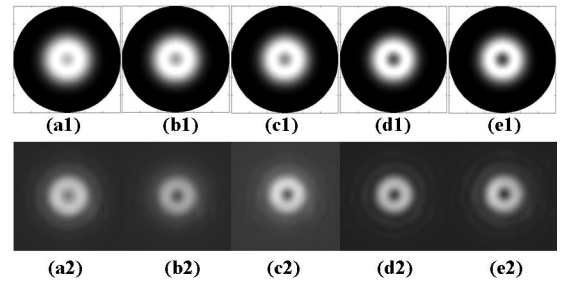


Fig. 4. The light intensity of partially coherent vortex beams from LED for different coherent lengths with the same topological charge ($l = 1$). (a₁)–(e₁): theoretical simulation; (a₂)–(e₂): experimental observation. Coherent lengths are (a₁) and (a₂): $\delta = 0.4292$ mm; (b₁) and (b₂): $\delta = 0.4811$ mm; (c₁) and (c₂): $\delta = 0.5244$ mm; (d₁) and (d₂): $\delta = 0.7068$ mm; (e₁) and (e₂): $\delta = 0.7808$ mm.

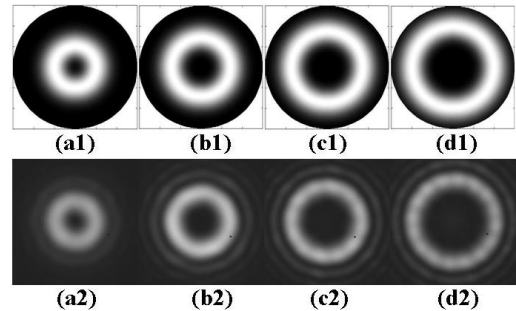


Fig. 5. The light intensity of partially coherent vortex beams from LED for four different topological charges with the same coherent length ($\delta = 0.7068$ mm) (a₁)–(d₁) theoretical simulation; (a₂)–(d₂) experimental observation. Topological charges are (a₁) and (a₂) $l = 2$; (b₁) and (b₂) $l = 4$; (c₁) and (c₂) $l = 6$; (d₁) and (d₂) $l = 8$.

In this section, we have presented theoretical simulations and their corresponding experimental observations to show the properties of partially coherent vortex beams from LED. Particular interest is paid to the effects of coherent length, topological charge and propagation distance on intensity of partially coherent vortex beams.

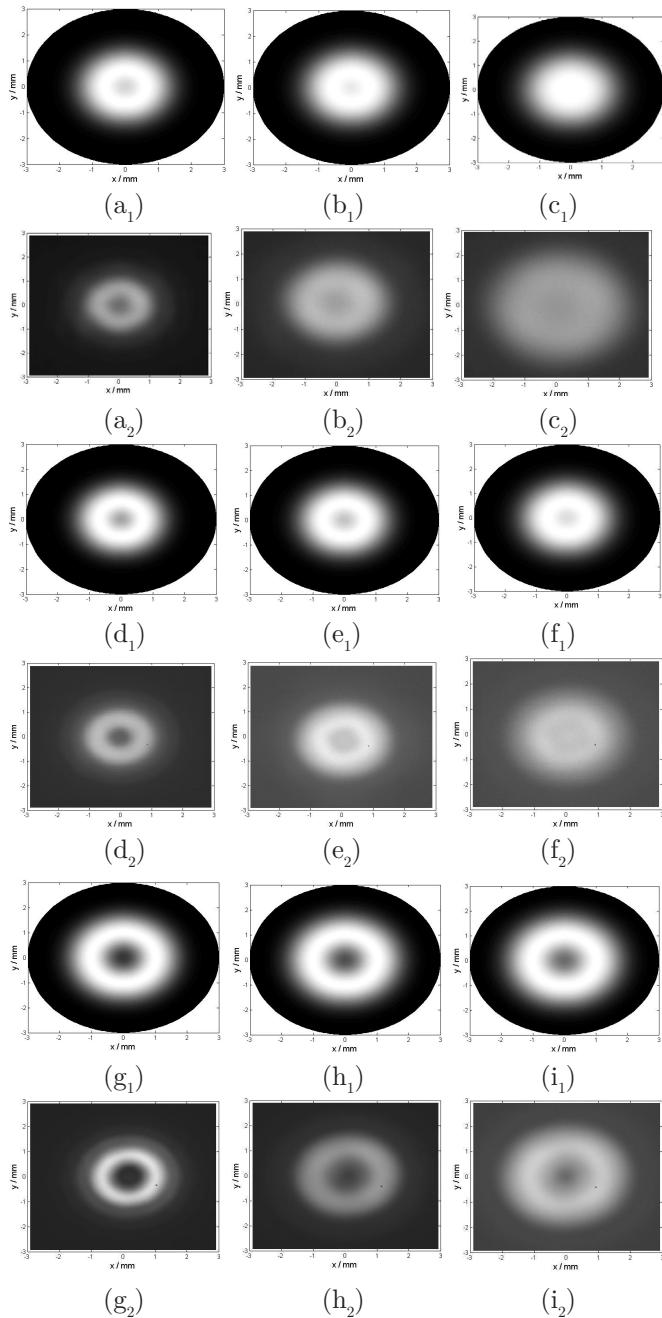


Fig. 6. Theoretical simulations (a₁)–(i₁) and their corresponding experimental observations (a₂)–(i₂) of the light intensity of partially coherent vortex beams from LED in different propagation distances. Topological charges are (a₁)–(f₁) $l = 1$; (g₁)–(i₁) $l = 2$. Coherent lengths are (a₁)–(c₁) $\delta = 0.4292$ mm; (d₁)–(i₁) $\delta = 0.7068$ mm. Propagation distances are (a₁) $z = 10$ cm; (b₁) $z = 25$ cm; (c₁), (d₁) and (g₁) $z = 50$ cm; (e₁) and (h₁) $z = 75$ cm; (f₁) and (i₁) $z = 100$ cm.

Partially coherent vortex beams with different coherent lengths are obtained by adjusting the position of the aperture, SPP and CCD. Table 1 shows the coherent length with corresponding distance between the LED and the aperture.

Figure 4 shows the intensity distribution of partially coherent vortex beams with topological charge $l = 1$. With the increment of coherent length, the intensity in the central dark region decreases, while the diameter of the aperture remains same. The experimental observations (a₂)–(e₂) coincide with the theoretical simulations (a₁)–(e₁). Besides, the rings around the beams in our experimental observations are attributed to the diffraction effects of the aperture.

Figure 5 shows the patterns of partially coherent vortex beams with coherent length $\delta = 0.7068$ mm. With the increment of topological charge, the central intensity reduces; meanwhile, the diameter of the beam increases. The diffraction rings can also be observed in our experiment.

Figure 6 presents the intensity of partially coherent vortex beams from LED during their propagation. The beam has a well-defined dark core in a short propagation distance. With an increase in the propagation distance, the dark core of the beam fills with light. In Fig. 7, the normalized intensity ($I(x, 0, z)/I(x, 0, z)_{max}$) distributions of partially coherent vortex beams from

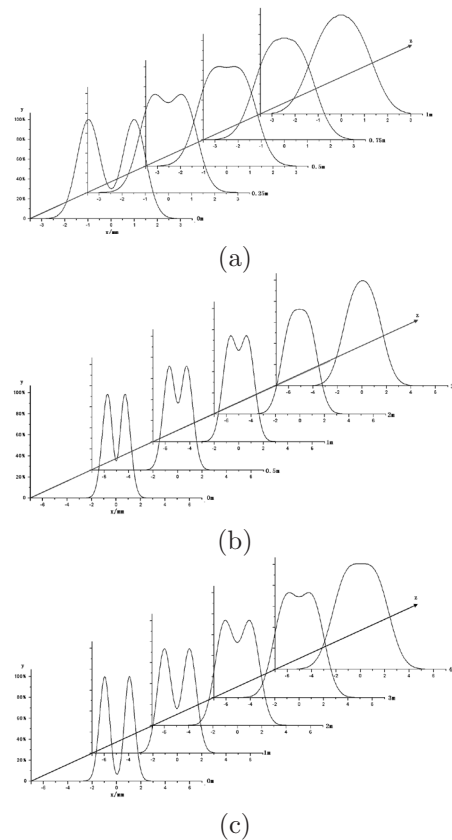


Fig. 7. Normalized intensity distribution at several selected distances of partially coherent vortex beams from LED for different coherent lengths (δ) or topological charges (l). (a) $\delta = 0.4292$ mm, $l = 1$; (b) $\delta = 0.7068$ mm, $l = 1$; (c) $\delta = 0.7068$ mm, $l = 2$.

LED in free-space propagation are plotted. It can be observed from these figures that with an increase in propagation distance, the intensity profile evolves from a central-dipped shape to a flat-topped shape and finally to a Gaussian shape. Furthermore, compared with the figures, the distance needed for the intensity profile to evolve as a Gaussian shape is longer for a higher coherent length or a larger topological charge of partially coherent vortex beams.

In conclusion, both theoretical analyses and experiments are conducted to investigate the generation and propagation of partially coherent vortex beams from LED. A dark hollow beam is obtained through a short-propagating distance. Meanwhile, the intensity of the dark core decreases with an increase in coherent length or topological charge. It is worthy to point out that the generated dark hollow beam evolves into a Gaussian beam through a certain distance, in which the propagating distance is increased by either a higher-order coherent length or a larger topological charge. This method may pave a new way to generate partially coherent vortex beams by using LEDs.

This research was supported by the National Natural Science Foundations of China (No. 61178015).

References

1. L. Allen, M. W. Beijersbergen, R. J. C. Spreeuw, and J. P. Woerdman, *Phys. Rev. A* **45**, 8185 (1992).
2. W. J. Firth and D. V. Skryabin, *Phys. Rev. Lett.* **79**, 2450 (1997).
3. J. Courtial, K. Dholakia, D. A. Robertson, L. Allen, and M. J. Padgett, *Phys. Rev. Lett.* **80**, 3217 (1998).
4. L. Shi, L. Tian, and X. Chen, *Chin. Opt. Lett.* **10**, 120501 (2012).
5. L. Guo, Z. Tang, C. Liang, and Z. Tan, *Chin. Opt. Lett.* **8**, 520 (2010).
6. G. Molina-Terriza, J. P. Torres, and L. Torner, *Phys. Rev. Lett.* **88**, 13601 (2001).
7. G. Gibson, J. Courtial, M. Padgett, M. Vasnetsov, V. Pas'ko, S. Barnett, and S. Franke-Arnold, *Opt. Express* **12**, 5448 (2004).
8. C. Ziyang, Z. Guowen, R. Lianzhou, and P. Jixiong, *Chin. J. Lasers* **35**, 1063 (2008).
9. J. Wu and A. D. Boardman, *J. Mod. Opt.* **38**, 1355 (1991).
10. J. Wu, *J. Mod. Opt.* **37**, 671 (1990).
11. D. M. Palacios, I. D. Maleev, A. S. Marathay, and G. A. Swartzlander, Jr, *Phys. Rev. Lett.* **92**, 143905 (2004).
12. G. A. Swartzlander and J. Schmit Jr, *J. Phys. Rev. Lett.* **93**, 093901 (2004).
13. I. D. Maleev and G. A. Swartzlander, Jr, *J. Opt. Soc. Am. B* **25**, 915 (2008).
14. C. Ke, Z. Hongrun, and L. Bai-Da, *Acta Phys. Sin.* **59**, 246 (2010).
15. K. Cheng and L. Baida, *Modern Opt.* **56**, 1119 (2009).
16. L. Hua, Z. Chen, and J. Pu, *Acta Opt. Sin.* **31**, s100403 (2011).
17. K. Gao, L. Xu, R. Zheng, G. Chen, H. Zheng, and H. Ming, *Chin. Opt. Lett.* **8**, 45 (2010).
18. X. Liu and J. Pu, *Opt. Express* **19**, 26444 (2011).
19. H. Lin, H. Tao, M. He, J. Pu, and L. Rao, *Acta Opt. Sin.* **32**, 0323003 (2012).
20. A. M. Siegel, G. A. Shawa, *J. Model. Proc. SPIE* **5530**, 182 (2004).
21. G. Chen, F. Abou-Galala, Z. Xu, and B. M. Sadler, *Opt. Express* **16**, 15059 (2008).